PHYSICAL REVIEW D VOLUME 40, NUMBER 10 15 NOVEMBER 1989

Static solutions of SU(2)-Higgs theory

Laurence G. Yaffe
Department of Physics, FM-15, University of Washington, Seattle, Washington 98195
(Received 26 June 1989)

The structure and stability of static spherically symmetric solutions in the SU(2)-Higgs theory are examined using both analytic and numerical methods. Accurate results are presented for the energy and instability growth rates of the "sphaleron" solution as a function of the Higgs-boson mass. The sphaleron is shown to undergo an infinite sequence of bifurcations as the Higgs-boson mass is increased, starting at $M_H = 12 M_W$. New "deformed sphaleron" solutions emerge from each of these bifurcations. These deformed sphalerons are not charge-conjugation invariant, have non-half-integral winding numbers, and are lower in energy than the original sphaleron. Hence, for sufficiently large Higgs-boson mass, minimal-energy paths connecting inequivalent vacuum states do not pass through the original sphaleron configuration.

I. INTRODUCTION

The existence of a static spherically symmetric solution, commonly called the "sphaleron," in the SU(2) gauge theory with a fundamental-representation Higgs field has been known for many years.[1] A plausible interpretation of this solution was provided by the suggestion that the sphaleron describes the top of the potential-energy barrier separating gauge-inequivalent classical vacua.[2] (More precisely, the "top of the barrier" means the highest-energy configuration on a minimal-energy path connecting inequivalent vacua.[3,4]) This interpretation underlies the recent discussion of electroweak baryon-number violation produced by thermally activated formation and subsequent decay of sphaleron configurations (for example, Refs. 5–7).

The exact structure of the sphaleron solution cannot be determined analytically. Nevertheless, numerous people have used numerical or variational techniques to estimate various properties of the sphaleron.[8,2,6] However, the small fluctuation spectrum of the sphaleron has not yet been computed and, in particular, the number of instabilities of the sphaleron has not been fully determined. This is an important question as it bears directly on the interpretation of the sphaleron as the top of the potential-energy barrier. The highest-energy point on a minimal-energy path connecting inequivalent vacua must be a classical solution with a single direction of instability, i.e., a saddle point at which the curvature has a single negative eigenvalue.[9] (If more than one negative mode exists, then the putative minimal-energy path could be deformed to produce a new path with a smaller maximal energy—contradicting the original assumption of minimal energy.) Hence, if the sphaleron has more than a single unstable direction, then it is not the correct solution to use in the semiclassical calculation of finite-temperature baryon-number violation.

This paper examines static, spherically symmetric solutions in the SU(2)-Higgs theory using both analytic and numerical methods. In particular, accurate results for the energy and instability growth rates of the "sphaleron" solution are presented as a function of the Higgs-boson mass. The sphaleron is found to undergo an infinite sequence of bifurcations as the Higgs mass is increased, starting at $M_H = 12.03 M_W$. Below this mass, only a single direction of instability exists (for spherically symmetric deformations).[10] A second instability develops when M_H exceeds $12.03 M_W$, and further instabilities appear above $M_H = 138 M_W$. For a large Higgs mass, the number of negative curvature eigenvalues is proportional to $\ln(M_H/M_W)$.

Each passage through zero of a curvature eigenvalue indicates a bifurcation of the sphaleron from which new "deformed sphaleron" solutions emerge. These deformed sphalerons are not charge-conjugation invariant, have non-half-integral winding numbers, and are lower in energy than the original sphaleron. The nth bifurcation generates a branch of deformed solutions having n directions of instability. Solutions on the first branch of deformed sphalerons are lowest in energy and correctly characterize the top of the potential-energy barrier when the Higgs mass exceeds $12 M_W$. The fact that these solutions are not charge-conjugation invariant implies that there are two distinct minimal-energy paths (related by charge conjugation) connecting neighboring vacuum states.

The remainder of this paper is organized as follows.[11] Section II introduces our notation for the SU(2)-Higgs theory and summarizes the relevant topology for four-dimensional gauge fields. The general ansatz for spherically symmetric configurations is reviewed, and the restriction to static field configurations is described. The spherically symmetric subspace of the $(3+1)$-dimensional theory may be viewed as a $(1+1)$-dimensional theory of a U(1) gauge field coupled to two complex scalar fields;[12] this convenient form is used throughout the paper.

The classic sphaleron solution is examined in Sec. III. The sphaleron is a local minimum of the energy when restricted to charge-conjugation-invariant configurations. It may be viewed as a soliton of the effective $(1+1)$-dimensional theory. Analytic results on the asymptotic

behavior and instabilities of the sphaleron are described. Accurate numerical results are presented for the form, energy, and negative curvature eigenvalues of the sphaleron as a function of the Higgs mass.

Section VI is devoted to the "deformed" sphaleron solutions. Numerical results are presented for the structure, energy, and negative curvature eigenvalues of the first two branches of deformed sphalerons.

The extension of the spherically symmetric ansatz to include fermions, and a brief description of the numerical techniques used, are contained in two appendixes.

II. SU(2)-HIGGS THEORY

The SU(2)-Higgs theory may be defined by the action

$$S\equiv\frac{1}{g^2}\int d^4x\left[-\tfrac{1}{2}\mathrm{tr}(F_{\mu\nu}F^{\mu\nu})+(D_\mu\Phi)^\dagger(D^\mu\Phi)+(\lambda/g^2)(\Phi^\dagger\Phi-\tfrac{1}{2}g^2v^2)^2\right]. \tag{2.1}$$

The scalar field Φ is an SU(2) doublet with covariant derivative $D_\mu\equiv(\partial_\mu+A_\mu)$, where $A_\mu\equiv A_\mu^a(\tau^a/2i)$. $F_{\mu\nu}\equiv[D_\mu,D_\nu]$ is the SU(2) field strength. We use a spacelike metric in Minkowski space, $\eta_{\mu\nu}\equiv\mathrm{diag}(-,+,+,+)$. Hence, the definition (2.1), as well as our subsequent equations, are valid in both Minkowski and Euclidean space.[13]

The action (2.1) generates the equations of motion

$$-D^\mu F_{\mu\nu}=\tfrac{1}{4}[(D_\nu\Phi)^\dagger\tau^a\Phi-\Phi^\dagger\tau^a(D_\nu\Phi)]\tau^a, \tag{2.2a}$$

$$D^\mu D_\mu\Phi=\frac{2\lambda}{g^2}(\Phi^\dagger\Phi-\tfrac{1}{2}g^2v^2)\Phi \tag{2.2b}$$

(where $D_\nu F_{\mu\lambda}\equiv\partial_\nu F_{\mu\lambda}+[A_\nu,F_{\mu\lambda}]$). The (semiclassical) W- and Higgs-boson masses are

$$M_W=\tfrac{1}{2}gv \tag{2.3}$$

and

$$M_H=\sqrt{2\lambda}v,$$

respectively.

The topological charge of a gauge field configuration is defined as

$$Q\equiv-\frac{1}{32\pi^2}\int d^4x\,\epsilon^{\mu\nu\alpha\beta}\mathrm{tr}(F_{\mu\nu}F_{\alpha\beta}). \tag{2.4}$$

This is an integer provided the field strength vanishes at (spacetime) infinity. Since the charge density is the divergence of the topological charge current, $-(\epsilon^{\mu\nu\alpha\beta}/32\pi^2)\mathrm{tr}(F_{\mu\nu}F_{\alpha\beta})=\partial_\mu K^\mu$ with

$$K^\mu=-\frac{1}{16\pi^2}\epsilon^{\mu\nu\alpha\beta}\mathrm{tr}(A_\nu F_{\alpha\beta}-\tfrac{2}{3}A_\nu A_\alpha A_\beta), \tag{2.5}$$

the topological charge may also be expressed as a surface integral:

$$Q=\int d^3x\,K^0\Big|_{t=-\infty}^{t=+\infty}+\int dt\,d\Omega\,r^2K^r\Big|_{r=0}^{r=\infty}.$$

One may choose a gauge where the vector potential vanishes sufficiently rapidly at spatial infinity so that $r^2K^r\to0$ as $r\to\infty$. In such a gauge, the topological charge equals the difference in the "winding number" of the gauge field at $t=\pm\infty$,

$$Q=\left[\lim_{t\to\infty}-\lim_{t\to-\infty}\right]q(A(t)), \tag{2.6}$$

where the winding number $q(A)$ of any three-dimensional gauge field is defined as the integral of the Chern-Simons density K^0:

$$q(A)\equiv\int d^3x\,K^0=-\frac{1}{16\pi^2}\int d^3x\,\epsilon^{0ijk}\mathrm{tr}(A_iF_{jk}-\tfrac{2}{3}A_iA_jA_k). \tag{2.7}$$

The winding number q may be regarded as a coordinate in gauge-orbit space which measures the position of topologically inequivalent vacua. Under an arbitrary gauge transformation $\Omega(x)$ (which approaches a constant at spatial infinity), $A_i\to A_i^\Omega\equiv\Omega D_i\Omega^\dagger$ and the winding number becomes

$$q(A^\Omega)=q(A)+\nu(\Omega). \tag{2.8}$$

Here,

$$\nu(\Omega)\equiv-\frac{1}{24\pi^2}\int d^3x\,\epsilon^{0ijk}\mathrm{tr}[(\Omega^\dagger\partial_i\Omega)(\Omega^\dagger\partial_j\Omega)(\Omega^\dagger\partial_k\Omega)] \tag{2.9}$$

is the integer which measures the homotopy class of the gauge transformation Ω. Thus, the winding number q is invariant under all "proper" gauge transformations (transformations continuously connected to the identity), but changes by an integer under topologically nontrivial gauge transformations. When restricted to vacuum configurations the winding number is quantized, $q(\Omega\partial\Omega^\dagger)=\nu(\Omega)$; however, for nonvacuum configurations q may take on arbitrary real values.

A. Spherically symmetric configurations

In addition to the local SU(2) gauge invariance, the SU(2)-Higgs theory (2.1) is also invariant under a global SU(2) symmetry which mixes the doublet Higgs field Φ with its complex conjugate $-i\tau_2\Phi^*$. "Spherically symmetric" configurations are those for which an O(3) rotation of spatial directions may be compensated by a suitable combination of SU(2) gauge and SU(2) global transformations.[14] A convenient ansatz for the most general spherically symmetric configuration is given by[12,15]

$$\begin{aligned}A_0(x)&=[a_0(r,t)\tau\cdot\hat{\mathbf{x}}]/2i,\\ A_j(x)&=\{[\alpha(r,t)-1]e_j^1/r+\beta(r,t)e_j^2/r+a_1(r,t)e_j^3\}/2i,\\ \Phi(x)&=[\mu(r,t)+i\nu(r,t)\tau\cdot\hat{\mathbf{x}}]\xi,\end{aligned} \tag{2.10}$$

where the six arbitrary functions are all real and ξ is an arbitrary two-component complex unit vector. The matrix valued functions $\{e_j^k\}$ are defined as

$$e_i^1=(\tau\cdot\hat{\mathbf{x}}\tau_i-\hat{\mathbf{x}}_i)/i=(\epsilon_{ijk}\hat{\mathbf{x}}_k)\tau_j\ ,$$
$$e_i^2=\tau_i-\tau\cdot\hat{\mathbf{x}}\hat{\mathbf{x}}_i=(\delta_{ij}-\hat{\mathbf{x}}_i\hat{\mathbf{x}}_j)\tau_j\ ,$$
$$e_i^3=\tau\cdot\hat{\mathbf{x}}\hat{\mathbf{x}}_i=(\hat{\mathbf{x}}_i\hat{\mathbf{x}}_j)\tau_j\ ,$$

where $\hat{\mathbf{x}}$ is a unit three-vector in the radial direction. It will be convenient to introduce (1+1)-dimensional complex scalar fields $\chi\equiv\alpha+i\beta$ and $\phi\equiv\mu+i\nu$, and the (1+1)-dimensional field strength $f_{\mu\nu}=\partial_\mu a_\nu-\partial_\nu a_\mu$ (with μ and ν now two-dimensional indices). Two-dimensional covariant derivatives will be defined as

$$D_\mu\chi=(\partial_\mu-ia_\mu)\chi,\quad D_\mu\phi=(\partial_\mu-ia_\mu/2)\phi\ . \tag{2.11}$$

This ansatz preserves a U(1) subgroup of the SU(2) gauge group consisting of the transformations $\{\Omega=\exp[i\omega(r,t)\tau\cdot\hat{\mathbf{x}}/2]\}$. Under these transformations,

$$\chi\mapsto e^{i\omega}\chi,\quad \phi\mapsto e^{i\omega/2}\phi,\quad A_\mu\mapsto a_\mu+\partial_\mu\omega\ . \tag{2.12}$$

Using this ansatz, the SU(2) electric and magnetic fields are

$$E_i\equiv F_{i0}=\left[-\frac{1}{r}\mathrm{Re}(D_0\chi)e_i^1-\frac{1}{r}\mathrm{Im}(D_0\chi)e_i^2-f_{01}e_i^3\right]\Big/2i\ ,$$
$$B_i\equiv\tfrac{1}{2}\epsilon_{ijk}F_{jk}=\left[-\frac{1}{r}\mathrm{Im}(D_1\chi)e_i^1+\frac{1}{r}\mathrm{Re}(D_1\chi)e_i^2+\frac{1}{r^2}(|\chi|^2-1)e_i^3\right]\Big/2i\ .$$

The action, restricted to this ansatz, equals[16]

$$S=\frac{4\pi}{g^2}\int dt\,dr\left[\tfrac{1}{4}r^2f_{\mu\nu}f^{\mu\nu}+|D_\chi|^2+r^2|D\phi|^2-\mathrm{Re}(\chi^*\phi^2)+\frac{1}{2r^2}(|\chi|^2-1)^2+\tfrac{1}{2}(|\chi|^2+1)|\phi|^2+\frac{\lambda}{g^2}r^2(|\phi|^2-\tfrac{1}{2}g^2v^2)^2\right]\ . \tag{2.13}$$

Varying the reduced action (2.13) generates the (1+1)-dimensional field equations

$$-\partial^\mu(r^2f_{\mu\nu})=2\,\mathrm{Im}(\chi^*D_\nu\chi)+r^2\mathrm{Im}(\phi^*D_\nu\phi)\ , \tag{2.14a}$$
$$\left[-D^2+\frac{1}{r^2}(|\chi|^2-1)+\tfrac{1}{2}|\phi|^2\right]\chi=\tfrac{1}{2}\phi^2\ , \tag{2.14b}$$
$$\left[-D^\mu r^2D_\mu+\tfrac{1}{2}(|\chi|^2+1)+\frac{\lambda}{g^2}r^2(2|\phi|^2-g^2v^2)\right]\phi=\chi\phi^*\ . \tag{2.14c}$$

[These equations can also be derived by substituting the ansatz (2.10) directly into the (3+1)-dimensional equations of motion (2.2).]

Finite-energy solutions must satisfy

$$\chi\to e^{i\omega},\quad \phi\to e^{i\omega/2}(gv/\sqrt{2}),\quad a_\mu\to\partial_\mu\omega\ ,$$

and (2.15a)

$$D_\mu\chi\to0,\quad r\,D_\mu\phi\to0,\quad f_{\mu\nu}\to0\ ,$$

as $r\to\infty$. (Finite-action Euclidean solutions must also satisfy these boundary conditions as $t\to\pm\infty$.) At short distance, finiteness of the energy, the SU(2) field strength, and the gauge current requires that

$$|\chi|\to1,\quad \chi|\phi|^2\to\phi^2,\quad D_\mu\chi\to0\ , \tag{2.15b}$$

as $r\to0$. These conditions on the short-distance behavior imply that the $r=0$ singularities in the gauge potential and Higgs field may be removed by a suitable gauge transformation.

The topological charge density of configurations in this ansatz is

$$-\frac{1}{32\pi^2}\epsilon^{\mu\nu\alpha\beta}\mathrm{tr}(F_{\mu\nu}F_{\alpha\beta})=-\frac{1}{16\pi^2}\frac{\epsilon^{\mu\nu}}{r^2}[f_{\mu\nu}(1-|\chi|^2)-2i(D_\mu\chi)^*(D_\nu\chi)] \tag{2.16}$$

and the topological current is

$$K^0=-\frac{1}{8\pi^2r^2}\epsilon^{01}\left[a_1-\mathrm{Im}\partial_1\chi+\frac{1}{2i}[\chi^*(D_1\chi)-(D_1\chi)^*\chi]\right],$$
$$K^i=\frac{\hat{\mathbf{x}}^i}{8\pi^2r^2}\epsilon^{01}\left[a_0-\mathrm{Im}\partial_0\chi+\frac{1}{2i}[\chi^*(D_0\chi)-(D_0\chi)^*\chi]\right].$$

Hence, the topological charge equals

$$Q=-\frac{1}{4\pi}\int dt\,dr\,\epsilon^{\mu\nu}[f_{\mu\nu}(1-|\chi|^2)-2i(D_\mu\chi)^*(D_\nu\chi)]\ , \tag{2.17}$$

and the winding number $q=\int d^3x\,K^0$ is

$$q=-\frac{1}{2\pi}\int dr\,\epsilon^{01}\left[a_1-\mathrm{Im}\partial_1\chi+\frac{1}{2i}[\chi^*(D_1\chi)-(D_1\chi)^*\chi]\right]. \tag{2.18}$$

The boundary conditions (2.15) ensure the quantization of topological charge for finite action Euclidean configurations, and cause the (3+1)-dimensional topological charge to reduce to the simple flux integral which gives the usual topological charge in a (1+1)-

dimensional Abelian Higgs theory,

$$Q=-\frac{1}{4\pi}\int dt\,dr\,\epsilon^{\mu\nu}f_{\mu\nu}\ ,$$

or the equivalent form which measures the winding in the phase of the Higgs field:

$$Q=\frac{i}{4\pi}\int dr\,\epsilon^{01}[\chi^*(\partial_1\chi)-(\partial_1\chi)^*\chi]\Big|_{t=-\infty}^{t=+\infty}$$
$$-\frac{i}{4\pi}\int dt\,\epsilon^{01}[\chi^*(\partial_0\chi)-(\partial_0\chi)^*\chi]\Big|_{r=0}^{r=\infty}\ .$$

B. Static configurations

Arbitrary (spherically symmetric) field configurations which are static [up to a U(1) gauge transformation, (2.12)] may be expressed as a gauge transform of a strictly static configuration with $a_1=0$:

$$\begin{aligned}\chi(r,t)&=e^{i\omega(r,t)}\bar{\chi}(r)\ ,\\ \phi(r,t)&=e^{i\omega(r,t)/2}\bar{\phi}(r)\ ,\\ a_0(r,t)&=\partial_0\omega(r,t)+\bar{a}_0(r)\ ,\\ a_1(r,t)&=\partial_1\omega(r,t)\ .\end{aligned}\tag{2.19}$$

The energy of such a static configuration is[17]

$$E=\frac{4\pi}{g^2}\int dr\left[\tfrac{1}{2}r^2(\partial_r\bar{a}_0)^2+\bar{a}_0^2(|\bar{\chi}|^2+\tfrac{1}{4}r^2|\bar{\phi}|^2)\right.$$
$$+|\partial_r\bar{\chi}|^2+r^2|\partial_r\bar{\phi}|^2+\frac{1}{2r^2}(|\bar{\chi}|^2-1)^2$$
$$+\tfrac{1}{2}(|\bar{\chi}|^2+1)|\bar{\phi}|^2-\mathrm{Re}(\bar{\chi}^*\bar{\phi}^2)$$
$$\left.+\frac{\lambda}{g^2}r^2(|\bar{\phi}|^2-\tfrac{1}{2}g^2v^2)^2\right]\ .\tag{2.20}$$

The field equations (2.14) reduce to Gauss's law

$$(-\partial_r r^2\partial_r+2|\bar{\chi}|^2+\tfrac{1}{2}r^2|\bar{\phi}|^2)\bar{a}_0=0\tag{2.21a}$$

and a pair of coupled equations for the scalar fields:

$$\left[-\partial_r^2+\bar{a}_0^2+\frac{1}{r^2}(|\bar{\chi}|^2-1)+\tfrac{1}{2}|\bar{\phi}|^2\right]\bar{\chi}=\tfrac{1}{2}\bar{\phi}^2\ ,\tag{2.21b}$$

$$\left[-\partial_r r^2\partial_r+\tfrac{1}{4}r^2\bar{a}_0^2+\tfrac{1}{2}(|\bar{\chi}|^2+1)\right.$$
$$\left.+\frac{\lambda}{g^2}r^2(2|\bar{\phi}|^2-g^2v^2)\right]\bar{\phi}=\bar{\chi}\bar{\phi}^*\ .\tag{2.21c}$$

[The remaining gauge field equation in (2.14a) becomes a requirement of vanishing charge current, $2\,\mathrm{Im}(\bar{\chi}^*\partial_r\bar{\chi})+r^2\mathrm{Im}(\bar{\phi}^*\partial_r\bar{\phi})=0$. This, however, is an automatic consequence of the scalar equations (2.21b) and (2.21c) plus the boundary conditions (2.15b).] Since the linear operator in (2.21a) is strictly positive, Gauss's law requires the gauge field $\bar{a}_0$ to vanish for all static solutions.

The lowest-energy state is obviously $\bar{\phi}=gv/\sqrt{2}$ and $\bar{\chi}=1$. Vacuum configurations are given by arbitrary gauge transformations of this state, (2.19). If the phase difference of $\chi(r)$ between $r=0$ and ∞ is fixed at zero, then there is an infinite set of topologically inequivalent vacuum configurations distinguished by the winding number of the phase of the complex scalar field χ, $(i/2)\int_0^\infty dr[(\partial_r\chi)^*\chi-\chi^*(\partial_r\chi)]=2\pi n$, or equivalently by the line integral of the gauge field, $\int_0^\infty dr\,a_1=2\pi n$. These are just the classical "n-vacua" of an SU(2) gauge theory.[18,19]

III. THE SPHALERON

The sphaleron solution may be easily found by imposing charge-conjugation invariance on the static ansatz (2.19). Charge conjugation (or CP) transforms the scalar fields $\bar{\chi}$ and $\bar{\phi}$ into their complex conjugates and changes the sign of $\bar{a}_\mu$. Hence, static, spherically symmetric, charge-conjugation-invariant solutions are completely described by two real functions $\bar{\chi}(r)$ and $\bar{\phi}(r)$. The energy of such a configuration is

$$E=\frac{4\pi}{g^2}\int dr\left[(\partial_r\bar{\chi})^2+r^2(\partial_r\bar{\phi})^2+\frac{1}{2r^2}(\bar{\chi}^2-1)^2\right.$$
$$\left.+\tfrac{1}{2}(\bar{\chi}-1)^2\bar{\phi}^2+\frac{\lambda}{g^2}r^2(\bar{\phi}^2-\tfrac{1}{2}g^2v^2)^2\right]\tag{3.1}$$

and the equations of motion reduce to the pair of coupled equations:

$$\left[-\partial_r^2+\frac{1}{r^2}(\bar{\chi}^2-1)+\tfrac{1}{2}\bar{\phi}^2\right]\bar{\chi}=\tfrac{1}{2}\bar{\phi}^2\ ,\tag{3.2a}$$

$$\left[-\partial_r r^2\partial_r+\tfrac{1}{2}(\bar{\chi}-1)^2+\frac{\lambda}{g^2}r^2(2\bar{\phi}^2-g^2v^2)\right]\bar{\phi}=0\ .\tag{3.2b}$$

(These are equivalent to the equations of Ref. 2.)

For charge-conjugation-invariant static configurations, the boundary conditions (2.15) imply that $\bar{\chi}=1$ at $r=\infty$ and $\bar{\chi}=\pm1$ at $r=0$. The sphaleron is the lowest-energy configuration in which $\bar{\chi}$ moves from -1 at $r=0$ to $+1$ at $r=\infty$.

To calculate the winding number of the sphaleron, one should choose a gauge in which $\chi(0)=\chi(\infty)$. (Otherwise, field configurations which interpolate between a classical n vacuum and the sphaleron will have nonzero topological current flowing in from the spatial boundaries.) Since $\bar{\chi}(0)=-\bar{\chi}(\infty)$, a suitable gauge transformation will change the phase difference between $\bar{\chi}(0)$ and $\bar{\chi}(\infty)$ by $2\pi(n+\frac{1}{2})$. The resulting winding number, (2.18), simply measures this phase difference $q_{\mathrm{sph}}=n+\frac{1}{2}$. Hence, sphaleron solutions sit "midway" between adjacent classical vacua.

A. Sphaleron structure

It does not appear possible to solve the coupled equations (3.2) analytically. However, the asymptotic behavior of the sphaleron solution at short and long distance may be easily determined.

As r approaches 0, $\bar{\chi}(r)\to -1$ and $\bar{\phi}(r)\to 0$. $\bar{\chi}$ may be expanded in an even-power series,

$$\bar{\chi}(r)=-1+a_2 r^2+a_4 r^4+\cdots ,$$

while $\bar{\phi}$ has an odd expansion:

$$\bar{\phi}(r)=b_1 r+b_3 r^3+\cdots .$$

Inserting these expansions into the sphaleron equations (3.2) yields recurrence relations which may be used to express all power-series coefficients in terms of the lowest two coefficients a_2 and b_1. These two coefficients, however, can only be determined by integrating the solution from $r=0$ to $r=\infty$ and using the large-distance boundary conditions.[2]

As $r\to\infty$, $\bar{\chi}(r)\to 1$ and $\bar{\phi}(r)\to gv/\sqrt{2}$. To find the precise asymptotic behavior it is convenient to write

$$\bar{\phi}(r)=\frac{gv}{\sqrt{2}}\left[1-\frac{\eta(r)}{r}\right] \tag{3.3}$$

and to reexpress (3.2) as

$$\left[-\partial_r^2+\frac{1}{r^2}(\bar{\chi}+1)\bar{\chi}+M_W^2(1-\eta/r)^2\right](\bar{\chi}-1)=0 ,$$

$$[-\partial_r^2+M_H^2(1-\eta/r)(1-\eta/2r)]\eta=\frac{1}{2r}(\bar{\chi}-1)^2(1-\eta/r) .$$

In this form, one can readily show that

$$\eta(r)=\frac{[\bar{\chi}(r)-1]^2}{2M_H^2 r}[1+O(1/M_H^2 r^2)]+O(e^{-M_H r}/M_H) , \tag{3.4a}$$

$$\bar{\chi}(r)=1-ce^{-M_W r}\left[1+\frac{1}{M_W r}\right][1+O(e^{-M_W r},e^{-M_H r})] . \tag{3.4b}$$

(c is an undetermined constant.) The deviation of $\bar{\phi}(r)$ from its vacuum expectation value is $O(e^{-M_H r}/M_H r)$ if $M_H<2M_W$ and $O(e^{-2M_W r}/M_H^2 r^2)$ if $M_H>2M_W$.

To determine the structure of the sphaleron completely, one must minimize the energy functional (3.1) numerically. This is fairly straightforward. Figure 1 is a plot of the solutions $\bar{\chi}$ and $\bar{\phi}$ for several values of the mass ratio M_H/M_W. Note that the diameter of the sphaleron is 2–3 times M_W^{-1} (using the surface where $\chi=0$ as the "edge" of the sphaleron).

The energy of the sphaleron solution as a function of the Higgs-boson mass is shown in Fig. 2. The dependence on the Higgs mass is rather weak; if M_H lies between $\frac{1}{2}M_W$ and $5M_W$ then $E_{\rm sph}=4M_W/\alpha_W$ to within $\sim 15\%$. Table I shows a selection of this data in tabular form.[20] As $M_H\to\infty$, the sphaleron solution approaches a solution of the massive SU(2) gauge theory. In this limit, $\bar{\phi}(r)$ is fixed to its vacuum expectation value $\sqrt{2}M_W$, $\bar{\chi}(r)$ is the solution to $[-\partial_r^2+(\bar{\chi}+1)\bar{\chi}/r^2+M_W^2](\bar{\chi}-1)=0$, and the energy approaches $E_{\rm sph}=5.410M_W/\alpha_W$.

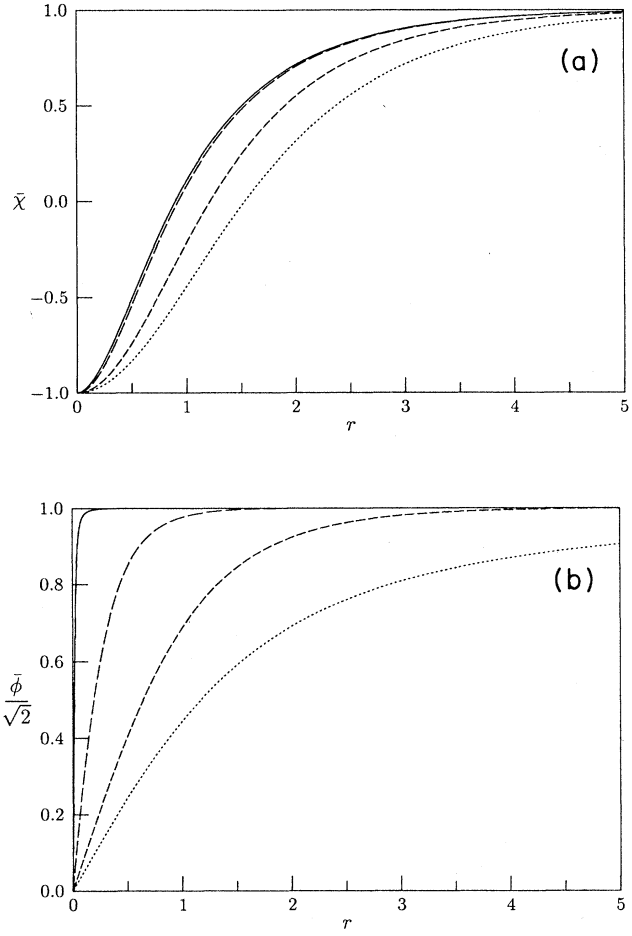

FIG. 1. Radial dependence of the fields $\bar{\chi}$ and $\bar{\phi}$ in the sphaleron. $\bar{\phi}$ and r^{-1} are measured in units of M_W. Shown are results for $M_H=0.1M_W$ (dotted curves), $M_H=M_W$ (short-dashed curve), $M_H=10M_W$ (long-dashed curve), and $M_H=100M_W$ (solid curves).

B. Sphaleron instabilities

The sphaleron is a local minimum of the energy functional (3.1) describing spherically symmetric, charge-conjugation-invariant configurations. It is, however, only a saddle point of the complete energy functional; perturbing the sphaleron by a charge-conjugation-odd fluctuation may lower its energy. This is easily shown by examining the second-order variation of the energy (2.20) expanded about the sphaleron solution. Since any gauge transformation of the sphaleron is also a solution, the small fluctuation describing a linearized U(1) global gauge transformation $\delta\bar{\chi}=i\bar{\chi}$ and $\delta\bar{\phi}=i\bar{\phi}/2$ (with $\delta\bar{a}_\mu=0$) is guaranteed to be a zero mode of the second-order small fluctuation operator $\delta^2 E$. This zero mode has one node in $\delta\bar{\chi}$ since $\bar{\chi}(r)$ changes sign. Consider modifying the fluctuation to remove this sign change, $\delta\bar{\chi}\equiv i|\bar{\chi}|$ and $\delta\bar{\phi}\equiv i\bar{\phi}/2$. Insertion of the absolute value sign only makes a difference in the single term of the energy (2.20),

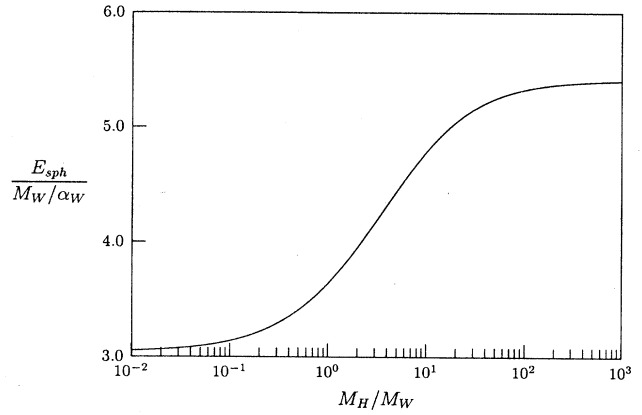

FIG. 2. Sphaleron energy (in units of M_W/α_W) as a function of the Higgs mass.

$-2\,\mathrm{Re}(\delta\bar{\chi}^*\delta\bar{\phi}\,\bar{\phi})=-|\bar{\chi}|\bar{\phi}^2$. Consequently, this fluctuation produces a second-order change in the energy,

$$\delta^2E=-\frac{4\pi}{g^2}\int dr(|\bar{\chi}|-\bar{\chi})\bar{\phi}^2\ ,$$

which is strictly negative. This proves that the sphaleron has at least one direction of instability.[21]

To determine if multiple instabilities exist, one must diagonalize the curvature δ^2E. Spherically symmetric instabilities can only appear in the subspace of charge-conjugation-odd, time-reversal-invariant fluctuations described by $\mathrm{Im}\delta\bar{\chi}(r)$ and $\mathrm{Im}\delta\bar{\phi}(r)$. In this sector, the curvature has the form

$$\delta^2E=\frac{4\pi}{g^2}\int dr\begin{bmatrix}\mathrm{Im}\delta\bar{\chi}\\ r\,\mathrm{Im}\delta\bar{\phi}\end{bmatrix}^T\mathcal{M}\begin{bmatrix}\mathrm{Im}\delta\bar{\chi}\\ r\,\mathrm{Im}\delta\bar{\phi}\end{bmatrix}\ ,$$

where

TABLE I. Sphaleron energy and negative curvature eigenvalues for different values of the Higgs-boson mass.

$\frac{M_H}{M_W}$	$\frac{E_{\rm sph}}{M_W/\alpha_W}$	$\frac{-\omega^2}{M_W^2}$			
0.00	3.0405	1.318			
0.01	3.0517	1.338			
0.02	3.0624	1.356			
0.05	3.0926	1.408			
0.07	3.1115	1.440			
0.1	3.1384	1.486			
0.2	3.2188	1.626			
0.3	3.2892	1.752			
0.5	3.4099	1.979			
0.7	3.5121	2.182			
1.0	3.6417	2.460			
1.5	3.8151	2.877			
2.0	3.9532	3.257			
3.0	4.1633	3.967			
4.0	4.3179	4.667			
5.0	4.4375	5.405			
7.0	4.6115	7.176			
10.0	4.7805	11.21			
15.0	4.9450	23.43	0.947		
20.0	5.0417	42.80	2.018		
30.0	5.1504	101.1	3.229		
50.0	5.2473	291.8	4.740		
70.0	5.2919	579.5	6.206		
100.0	5.3267	1 192	9.304		
150.0	5.3545	2 694	19.18	0.402	
200.0	5.3687	4 798	35.81	1.667	
300.0	5.3831	10 811	87.10	2.996	
500.0	5.3948	30 054	256.0	4.485	
700.0	5.3998	58 920	511.3	5.809	
1000.0	5.4036	120 259	1 055	8.418	
1500.0	5.4065	270 603	2 389	16.51	0.040
2000.0	5.4080	481 084	4 257	30.49	1.377

$$\mathcal{M}\equiv\begin{bmatrix}-\partial_r^2+(\bar{\chi}^2-1)/r^2+\frac{1}{2}\bar{\phi}^2 & -\bar{\phi}/r\\ -\bar{\phi}/r & -\partial_r^2+(\bar{\chi}+1)^2/2r^2+\lambda(2\bar{\phi}^2-g^2v^2)/g^2\end{bmatrix}\ . \tag{3.5}$$

Each eigenvector of $\mathcal{M}$ with a negative eigenvalue,

$$\mathcal{M}\begin{bmatrix}\mathrm{Im}\delta\bar{\chi}\\ r\,\mathrm{Im}\delta\bar{\phi}\end{bmatrix}=-\omega^2\begin{bmatrix}\mathrm{Im}\delta\bar{\chi}\\ r\,\mathrm{Im}\delta\bar{\phi}\end{bmatrix}\ , \tag{3.6}$$

generates an exponentially growing instability, $\delta\bar{\chi},\delta\bar{\phi}\propto e^{\omega t}$.

Accurately diagonalizing the curvature operator is somewhat more difficult than just solving for the sphaleron solution; however, it may be performed using standard numerical techniques. (See Appendix B for details.) Figure 3 plots the negative eigenvalues of the curvature as a function of Higgs-boson mass. For sufficiently small Higgs mass, only a single negative mode exists. However, a second negative mode appears at $M_H=12.03M_W$, and further instabilities appear at $M_H=138.3M_W$ and $1490M_W$. This is the beginning of an infinite sequence; for a large Higgs mass, the number of instabilities is proportional to $\ln(M_H/M_W)$.

These instabilities at a large Higgs-boson mass arise from the behavior of the curvature operator $\mathcal{M}$ when $M_H^{-1}\ll r\ll M_W^{-1}$. To see this, first write the curvature operator as

$$\mathcal{M}\equiv\begin{bmatrix}-\partial_r^2+(\bar{\chi}^2-1)/r^2 & 0\\ 0 & -\partial_r^2-2/r^2+(\bar{\chi}+1)^2/2r^2+\lambda(2\bar{\phi}^2-g^2v^2)/g^2\end{bmatrix}+\mathcal{K}\ ,$$

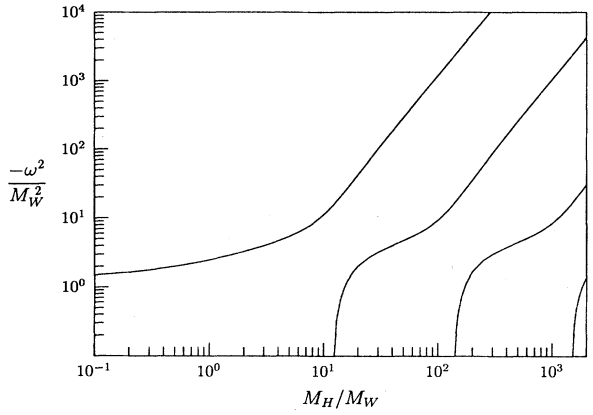

FIG. 3. Curvature of the unstable directions about the sphaleron as a function of the Higgs mass.

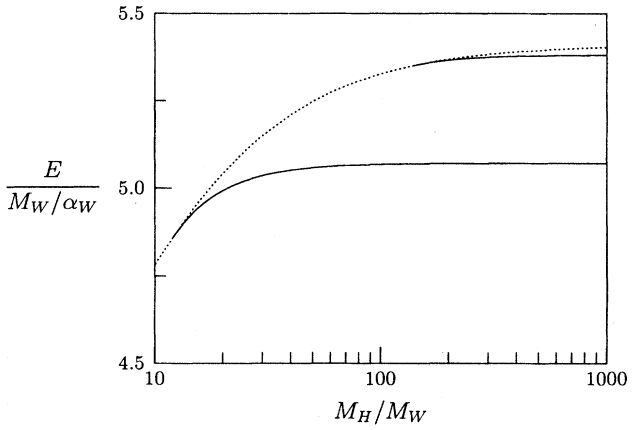

FIG. 4. Deformed sphaleron energies as a function of the Higgs mass. The solid lines show the energies of the first two branches of deformed solutions, while the dotted line indicates the original sphaleron energy.

where

$$\mathcal{K} \equiv \begin{bmatrix} \frac{1}{2}\bar{\phi}^2 & -\bar{\phi}/r \\ -\bar{\phi}/r & 2/r^2 \end{bmatrix},$$

and note that the eigenvalues of $\mathcal{K}$ are 0 and $\frac{1}{2}\bar{\phi}^2+2/r^2$. If $\mathcal{K}$ were replaced by its largest eigenvalue (times a 2×2 identity matrix), the number of negative modes could only decrease. Consequently, the number of negative modes of $\mathcal{M}$ is bounded below by the number of negative eigenvalues of the Schrödinger operator $-\partial_r^2+v(r)$, where

$$v(r)=\tfrac{1}{2}\bar{\phi}^2+(\bar{\chi}+1)^2/2r^2+\lambda(2\bar{\phi}^2-g^2v^2)/g^2 . \quad (3.7)$$

In the region $M_H^{-1} \ll r \ll M_W^{-1}$, we have $\bar{\chi}\simeq -1$, $\bar{\phi}\simeq\sqrt{2}M_W(1-2/M_H^2r^2)$, and

$$v(r)\simeq -\frac{2}{r^2}+M_W^2 . \quad (3.8)$$

One may easily show that the number of bound states in an attractive $1/r^2$ potential (with coefficient greater than $\frac{1}{4}$), confined to a region $r_{\min}<r<r_{\max}$, depends logarithmically on the ratio $r_{\max}/r_{\min}$. Since the $1/r^2$ form of the potential (3.7) is cut off at distances smaller than M_H^{-1} and larger than M_W^{-1}, one finds that the number of negative eigenvalues of $\mathcal{M}$ must grow logarithmically with increasing Higgs mass. A semiclassical calculation of the number of bound states in the potential (3.8) predicts that each increase in M_H/M_W by a factor of $e^{\pi/\sqrt{2}}=9.2$ will lead to the formation of one new negative eigenvalue. This agrees remarkably well with the numerical results.

IV. DEFORMED SPHALERONS

Each passage through zero of a small fluctuation eigenvalue of the sphaleron (at $M_H=12.03M_W$, $138.3M_W$, etc.) signals a bifurcation in the sphaleron solution. New branches of classical solutions appear at each bifurcation; the new solutions are not charge-conjugation invariant, have fewer directions of instability, and are lower in energy than the original sphaleron. The energy of these deformed sphalerons is shown in Fig. 4. The deformation of the sphaleron leading to the new solutions causes only a small change in energy (at most 8%); however, it produces a large change in the small fluctuation spectrum. The first branch of "deformed sphalerons" (starting at $12M_W$) is the lowest in energy and, as shown in Fig. 5, has a single negative eigenvalue of roughly constant magnitude. Each succeeding branch has one more direction of instability, so the nth branch of solutions has n negative eigenvalues.

Figure 6 shows the winding number of these solutions. The two outer branches of each "pitchfork" represent deformed solutions related by charge conjugation. For the first bifurcation, the deviation of the winding number

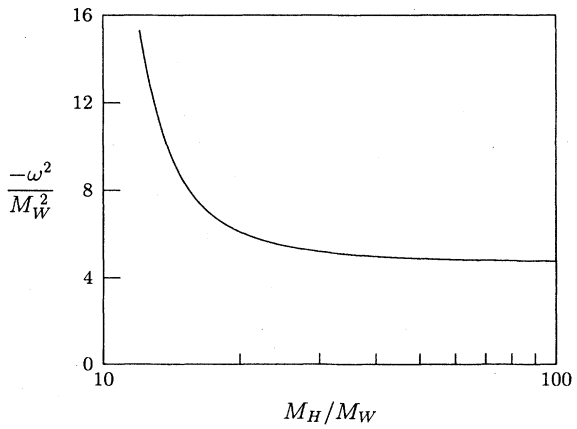

FIG. 5. Curvature of the unstable direction about the lowest-energy deformed sphaleron as a function of the Higgs mass.

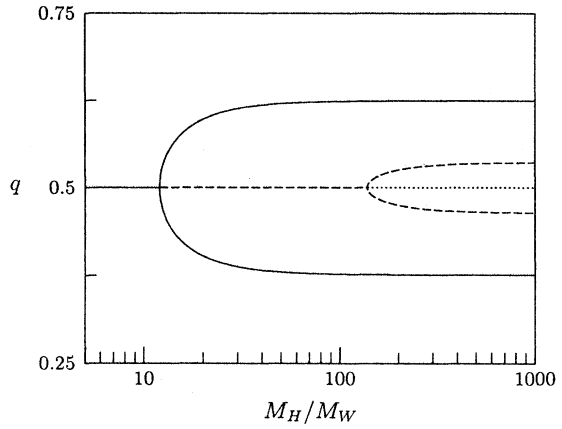

FIG. 6. Winding number q of sphaleron solutions as a function of the Higgs mass. Solid lines indicate solutions with a single direction of instability, dashed lines correspond to doubly unstable solutions, and dotted lines to triply unstable solutions.

from $\frac{1}{2}$ grows from zero at the bifurcation to ± 0.124 as $M_H \to \infty$.

The fields of the deformed sphalerons on the first two branches are shown in Fig. 7. The lack of charge-conjugation invariance in the deformed solution allows the Higgs field $\phi(r)$ to remain nonvanishing at the origin. This decreases the potential energy in the Higgs field, while increasing the kinetic energy due to the variation in phase of the Higgs field. For a sufficiently large Higgs mass, the loss of potential energy outweighs the increased kinetic energy; this is the basic mechanism causing the instability which leads to the formation of deformed sphalerons.

Tables II and III contain a selection of data on the first two branches of deformed sphalerons. The magnitude of the negative curvature eigenvalues monotonically decrease with increasing Higgs mass along both branches, and no additional bifurcations appear. In the limit of infinite Higgs mass, $M_H/M_W \to \infty$, the SU(2)-Higgs theory reduces to a gauged nonlinear sigma model and each deformed sphaleron becomes a classical solution of the gauged sigma model. The energy and negative curvature eigenvalues are finite and nonzero in this limit, and the deformed sphaleron fields remain nonsingular (even

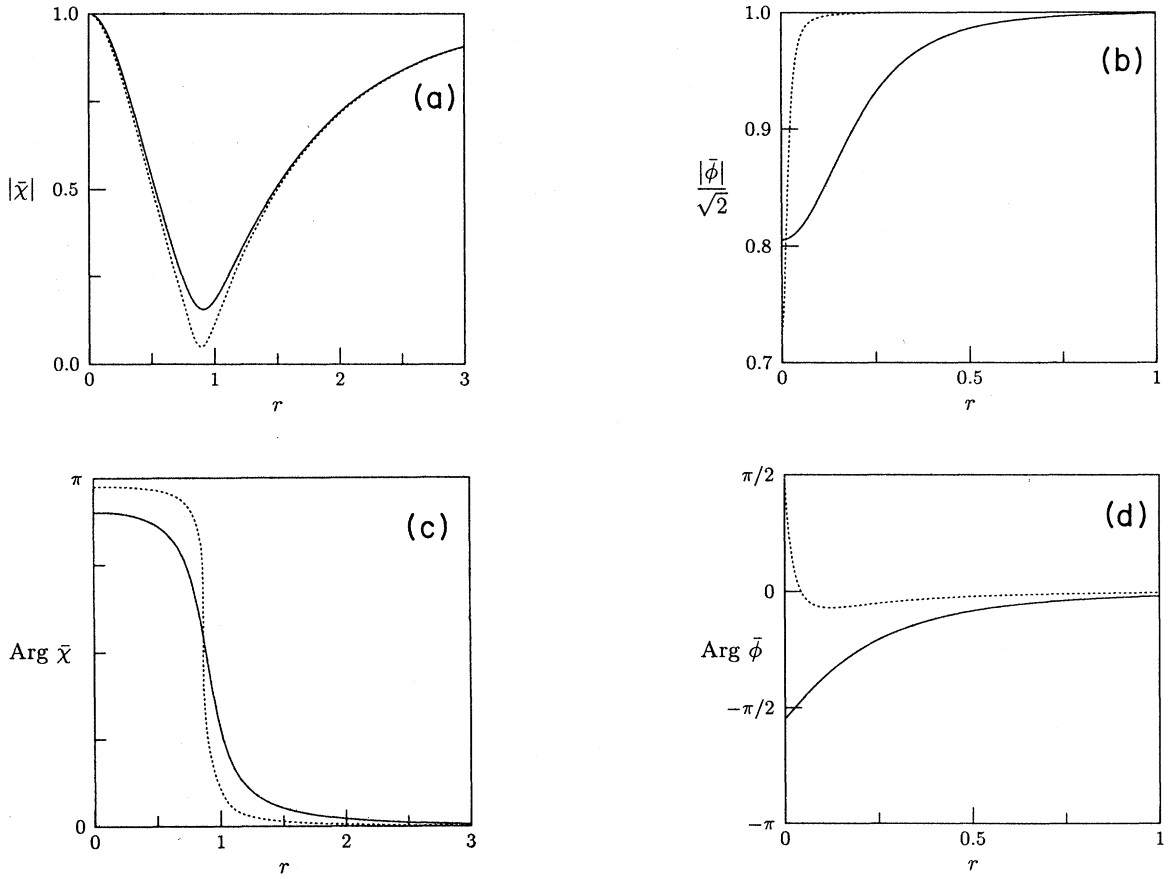

FIG. 7. Radial dependence of the fields $\bar{\chi}$ and $\bar{\phi}$ in the deformed sphaleron solutions. Shown are results for the lowest-energy deformed sphaleron at $M_H = 20 M_W$ (solid curves) and for the second branch solution at $M_H = 200 M_W$ (dotted curves). The first pair of plots shows the magnitude of the fields, while the second pair shows their phases. $|\bar{\phi}|$ and r^{-1} are measured in units of M_W.

TABLE II. Energy, winding number (q), and negative curvature eigenvalue (ω^2) for various values of the Higgs mass along the first branch of deformed sphalerons.

$\frac{M_H}{M_W}$	$\frac{E}{M_W/\alpha_W}$	q	$\frac{-\omega^2}{M_W^2}$
12.04	4.8598	0.495	15.235
13	4.8890	0.455	11.871
15	4.9333	0.428	8.439
20	4.9927	0.402	6.093
30	5.0357	0.387	5.201
50	5.0580	0.380	4.873
70	5.0642	0.378	4.793
100	5.0675	0.377	4.752
150	5.0693	0.376	4.731
200	5.0699	0.376	4.723
300	5.0703	0.376	4.718
500	5.0705	0.376	4.715
1000	5.0706	0.376	4.714
∞	5.0707	0.376	4.714

at the origin). The limiting energy of the first deformed sphaleron, $5.0707 M_W/\alpha_W$, agrees with earlier work on classical solutions in the gauged nonlinear sigma model.[22]

The presence of a unique direction of instability in the first branch of deformed sphalerons justifies their physical interpretation as the highest-energy configuration on a minimal-energy path connecting inequivalent classical vacua (assuming that no spherically asymmetric instabilities exist). The fact that the deformed sphaleron is not charge-conjugation invariant means that there are actually two distinct minimal-energy paths (related by charge conjugation) connecting neighboring classical vacua (when $M_H > 12 M_W$).

Note added. The existence of deformed sphaleron solutions was independently discovered by Kunz and Brihaye.[23] However, these authors did not study the negative eigenvalues of sphaleron solutions and mistakenly suggest that deformed sphalerons cannot be the maximal-energy configurations on noncontractable loops (i.e., paths connecting inequivalent vacua) because the Higgs field in these solutions is everywhere nonvanishing. This is incorrect. When the original sphaleron has multiple negative modes, deforming a noncontractable loop whose highest-energy point is the original sphaleron, in the direction of the second negative curvature mode, will decrease the maximal energy of configurations on the loop. At least in a neighborhood of the first bifurcation, the lowest-energy noncontractable loop produced by such a deformation will be one whose highest-energy configuration is the deformed sphaleron solution. A simple continuity argument, combined with the fact that the first deformed sphaleron is always the lowest-energy deformed sphaleron, then implies that deformed sphalerons on the first branch must continue to represent maximal-energy configurations on a noncontractable loops *provided* no totally new classical solution appears in a disjoint region of configuration space. (More picturesquely, the deformed sphaleron always represents the lowest-energy "pass" in the potential-energy barrier separating inequivalent vacua, provided this lowest-energy pass evolves continuously as the Higgs mass increases. However, if a new "mountain range" appears in the configuration space as the Higgs mass increases, then the maximal-energy configuration might jump discontinuously away from the known deformed sphaleron solutions.) No evidence suggesting the occurrence of such a discontinuity is known.

TABLE III. Energy, winding number (q), and negative curvature eigenvalue (ω^2) for various values of the Higgs mass along the second branch of deformed sphalerons.

$\frac{M_H}{M_W}$	$\frac{E}{M_W/\alpha_W}$	q		$\frac{-\omega^2}{M_W^2}$
138.3	5.3498	0.499	2285	16.22
140	5.3505	0.495	2187	15.45
150	5.3544	0.487	1719	12.07
200	5.3660	0.475	804.3	7.009
300	5.3747	0.468	502.4	5.673
500	5.3792	0.465	410.5	5.260
1000	5.3811	0.464	379.6	5.116
∞	5.3817	0.464	370	5.07

ACKNOWLEDGMENTS

Bharat Ratra and Lowell Brown are thanked for helpful conversations. This work was partially supported by the Department of Energy under Contracts Nos. DE-AC02-76ER03072 and DE-AS06-88ER40423. The author thanks the Alfred P. Sloan Foundation for financial support.

APPENDIX A: FERMIONS

Fermions may be added to the SU(2)-Higgs theory without destroying the global symmetry which permits the existence of nontrivial spherically symmetric configurations. Adding n_f left-handed SU(2)-doublet fermion fields $\{\Psi_L^I\}$ ($I=1,\ldots,n_f$) with action

$$S_{\text{ferm}} \equiv \frac{1}{g^2}\int d^4x (i\Psi_L^{I\dagger}\sigma^\mu D_\mu \Psi_L^I) , \tag{A1}$$

produces a theory which is identical to the full $\mathrm{SU}(2)_L \times \mathrm{U}(1)_Y$ electroweak theory in the limit in which $\theta_W = 0$ and all Yukawa couplings are set to zero. In this limit, the $\mathrm{U}(1)_Y$ gauge field and the right-handed SU(2) singlet fermions decouple and hence may be neglected.[24] (The spatial components of the 2×2 spin matrices σ^μ are ordinary Pauli matrices and the time component is defined to be -1 in Minkowski space, or $-i$ in Euclidean space.)

Spherically symmetric fermion fields are described by the ansatz

$$\Psi_L^I(x) = [f^I(r,t) + ig^I(r,t)\tau\cdot\hat{\mathbf{x}}]\Xi , \tag{A2}$$

where Ξ is the constant two-component spinor satisfying $\Xi^\dagger\Xi=1$ and $(\sigma+\tau)\Xi=0$ (which implies that $\Xi^\dagger\tau\Xi=0$).

The complex functions f^I and g^I may be conveniently combined to form (1+1)-dimensional Dirac fermions:

$$\psi^I \equiv r\begin{bmatrix} f^I \\ g^I \end{bmatrix} .$$

The fermion action then reduces to

$$S_{\rm ferm} \equiv \frac{4\pi}{g^2}\int dt\, dr\, \bar{\psi}^I\left[\gamma^\mu D_\mu + \frac{1}{r}(\mathrm{Re}\chi + i\gamma_5 \mathrm{Im}\chi)\right]\psi^I , \tag{A3}$$

where we have defined the two-dimensional gamma matrices $\gamma^0\equiv -i\sigma_1$, $\gamma^1\equiv -\sigma_3$, $\gamma^5\equiv\gamma^0\gamma^1=\sigma_2$, and use $\bar{\psi}\equiv\psi^\dagger(i\gamma^0)$. In this form, the one-dimensional fermions have an axial gauge coupling, $D_\mu\psi=(\partial_\mu+ia_\mu\gamma^5/2)\psi$, and transform as $\psi\to e^{-i\omega\gamma^5/2}\psi$ under the U(1) gauge transformation (2.12). Because of the factor of $1/r$ in the coupling to the Higgs field χ, finiteness of the energy requires that the fermion field ψ^I vanish as $r\to 0$.

The fermion-number current $J_I^\mu\equiv-\Psi_L^{I\dagger}\sigma^\mu\Psi_L^I$ is given by

$$\begin{aligned} J_I^0 &= \Psi_L^{I\dagger}\Psi_L^I = \frac{i}{r^2}\bar{\psi}^I\gamma^0\psi^I , \\ J_I^i &= -\Psi_L^{I\dagger}\sigma^i\Psi_L^I = i\frac{\hat{\mathbf{x}}^i}{r^2}\bar{\psi}^I\gamma^1\psi^I . \end{aligned} \tag{A4}$$

When quantized, the (1+1)-dimensional theory (A3) has anomalies in the fermion-number current $j_I^\mu\equiv 4\pi i\bar{\psi}^I\gamma^\mu\psi^I$ caused by axial-vector coupling to the two-dimensional (2D) gauge field:

$$\partial_\mu j_I^\mu = -\frac{g^2}{4\pi}\epsilon^{\mu\nu}f_{\mu\nu} . \tag{A5}$$

This does not equal the reduction of the four-dimensional anomaly equation,

$$\partial_\mu J_I^\mu = -\frac{g^2}{32\pi^2}\epsilon^{\alpha\beta\mu\nu}\mathrm{tr}(F_{\alpha\beta}F_{\mu\nu}) , \tag{A6}$$

since the right-hand side of (A5) differs from the four-dimensional topological charge density (2.16). This is because nonspherically symmetric components of the fermion field contribute to the local form of the anomaly. However [given the boundary conditions (2.15) in Euclidean space], the integrated forms of the 4D and 2D anomalies are identical:

$$\Delta N_I \equiv \frac{1}{g^2}\int d^4x\, \partial_\mu J_I^\mu = \frac{1}{g^2}\int d^2x\, \partial_\mu j_I^\mu = Q . \tag{A7}$$

This confirms the expectation that in spherically symmetric gauge fields, anomalous production of fermions is confined to the spherically symmetric partial wave.

In the field of a sphaleron, the Dirac equation, $[\gamma^\mu D_\mu+(\mathrm{Re}\chi+i\,\mathrm{Im}\chi\gamma_5)/r]\psi^I=0$, has one static zero mode for each fermion species.[25,26] The zero mode has the form

$$\psi(r,t)=e^{-i\omega(r,t)\gamma_5/2}\psi_0(r) ,$$

where $(\gamma^1\partial_r+\bar{\chi}/r)\psi_0(r)=0$. This has a normalizable solution,

$$\psi_0(r)=\exp\left[-\int_{r_0}^r dr'\frac{\bar{\chi}(r')}{r'}\right]\psi(r_0) , \tag{A8}$$

with $\gamma_1\psi(r_0)\equiv\psi(r_0)$. The sphaleron asymptotics (3.4) implies that $\psi_0(r)\sim r$ as $r\to 0$ and $\psi_0(r)\sim 1/r$ as $r\to\infty$.

APPENDIX B: NUMERICAL METHODS

The approach used to find static solutions and determine their instabilities was quite simple. To reduce the problem to a finite number of degrees of freedom, the radial integral and spatial derivatives in the energy functional (2.20) were discretized. The gradient and curvature of the discretized energy were computed exactly and a quadratically convergent Newton minimization procedure was used to locate stationary points of the energy. Explicit diagonalization of the curvature matrix yielded the small fluctuation frequencies. Using the result of a minimization at one value of the Higgs mass as the input to the calculation at a nearby mass value allowed solutions to be easily followed as M_H/M_W was varied. Calculations with different numbers of points in the discretization, ranging from 20 to 240, were used to control the systematic error of the discretization.

The only major subtlety concerns the choice of discretization. The sphaleron solutions depend on two length scales M_W^{-1} and M_H^{-1}. When these two lengths are very different, the differential equations (3.2) satisfied by the sphaleron become quite stiff. Furthermore, when $M_H\gg M_W$, instabilities develop on length scales ranging between M_H^{-1} and M_W^{-1}. Hence, to obtain accurate results for the curvature eigenvalues, variations in the fields on all length scales between M_H^{-1} and M_W^{-1} must be well described. The best results were obtained using a uniform discretization of the transformed radial variable:

$$s=\ln\left[\frac{1+M_H r}{1+M_W r}\right]\Big/\ln(M_H/M_W) .$$

This transformation maps the semi-infinite line $0\le r<\infty$ to the unit interval $0\le s<1$. Since $ds/dr\propto 1/[(r+M_W^{-1})(r+M_H^{-1})]$, when $M_H\gg M_W$ this transformation leads to a discretization in which the density of points is approximately uniform in r when $r<M_H^{-1}$, uniform in $\ln(r)$ when $M_H^{-1}<r<M_W^{-1}$, and uniform in $1/r$ when $r>M_W^{-1}$.

With this choice of discretization, the numerical results converge quite rapidly as the number of points in the discretization is increased. For M_H/M_W close to one, a 40-point discretization yields values for the energy, or negative eigenvalues, accurate to about one part in 10^4, while 80 points are needed to achieve comparable accuracy when M_H equals 1000 M_W. All digits of the results shown in Tables I–III are accurate.

[1]R. Dashen, B. Hasslacher, and A. Neveu, Phys. Rev. D **10**, 4138 (1974).
[2]F. Klinkhamer and N. Manton, Phys. Rev. D **30**, 2212 (1984).
[3]C. Taubes, Commun. Math. Phys. **86**, 257 (1982); **86**, 299 (1982).
[4]N. Manton, Phys. Rev. D **28**, 2019 (1983).
[5]V. Kuzmin, V. Rubakov, and M. Shaposhnikov, Phys. Lett. **155B**, 36 (1985).
[6]P. Arnold and L. McLerran, Phys. Rev. D **36**, 581 (1987).
[7]J. Ellis, R. Flores, S. Rudaz, and D. Seckel, Phys. Lett. B **194**, 241 (1987).
[8]J. Boguta, Phys. Rev. Lett. **50**, 148 (1983).
[9]S. Coleman, Nucl. Phys. **B298**, 178 (1988).
[10]Nonspherically symmetric instabilities are not expected to exist, but have not been studied.
[11]A preliminary version of this work appears in the Proceedings of the Theoretical Physics Institute Workshop on Baryon-Number Nonconservation in Electroweak Theory, Minneapolis, 1988 (unpublished).
[12]B. Ratra and L. Yaffe, Phys. Lett. B **205**, 57 (1988).
[13]This theory is equivalent to the bosonic sector of the standard $SU(2)_L \times U(1)_Y$ electroweak theory in the limit in which the weak mixing angle $\theta_W = \arctan(g'/g)$ is set to zero (Ref. 2). In this limit, the $U(1)_Y$ gauge field decouples and hence may be neglected. The experimental value of the weak mixing angle is small enough that a perturbative treatment of the effects of the $U(1)_Y$ current should be valid. Neglect of the U(1) field is required for the existence of nontrivial spherically symmetric solutions. Fermions are ignored in most of this paper since they only affect the dynamics when quantum fluctuations are included.
[14]This additonal SU(2) global symmetry is required for the existence of nontrivial spherically symmetric configurations. In the full electroweak theory, a nonzero value of the weak mixing angle destroys this global symmetry and produces spherically asymmetric deformations of the classical solutions of the SU(2)-Higgs theory.
[15]This ansatz differs from Ref. 12 by a field redefinition. The current choice simplifies some of the following expressions.
[16]The factor of r^2 in the kinetic energy of the effective Higgs field ϕ could be removed by redefining ϕ as $\tilde{\phi}/r$. This would slightly simplify the resulting equations of motion; however, it complicates the discussion of boundary conditions and asymptotics.
[17]This expression for the energy of a static configuration may be easily derived by starting with the gauge field Hamiltonian in a physical gauge (such as temporal, $A_0=0$, or radial, $A_r=0$) and inserting the form of a static configuration (2.19) suitably transformed to the chosen gauge.
[18]C. Callan, R. Dashen, and D. Gross, Phys. Lett. **63B**, 334 (1976).
[19]R. Jackiw and C. Rebbi, Phys. Rev. Lett. **37**, 172 (1976).
[20]Previous results for the sphaleron energy obtained using a variational ansatz (Ref. 2) agree quite well with our numerical results despite the fact that the variational ansatz of Ref. 2 has incorrect long-distance behavior for ϕ when $M_H > 2M_W$.
[21]J. Burzlaff, Nucl. Phys. **B233**, 262 (1984).
[22]G. Eilam, D. Klabucar, and A. Stern, Phys. Rev. Lett. **56**, 1331 (1986); G. Eilam and A. Stern, Nucl. Phys. **B294**, 775 (1987).
[23]J. Kunz and Y. Brihaye, Phys. Lett. B **216**, 353 (1989).
[24]Nonzero Yukawa couplings break the global symmetry needed for nontrivial spherically symmetric configurations. Omitting the Yukawa couplings corresponds to neglecting fermion masses; this should be a reasonable approximation when considering physics at temperatures well above the W-boson mass.
[25]C. Nohl, Phys. Rev. D **12**, 1840 (1975).
[26]J. Boguta and J. Kunz, Phys. Lett. **154B**, 1407 (1985).